



## Development of a shooting machine for the selection of arrows

メタデータ	言語: English 出版者: SAGE Publications Ltd 公開日: 2023-10-12 キーワード (Ja): キーワード (En): Archery, archer, archery player, arrow, shooting machine, arrow selection, olympic games, cluster analysis 作成者: Ohara, Masashi, Kawasaki, Naoki, Song, Hyunwoo, Shinojima, Ayane, Naka, Yuma, Takada, Yogo, Watanabe, Hitoshi メールアドレス: 所属:
URL	<a href="http://hdl.handle.net/10466/0002000060">http://hdl.handle.net/10466/0002000060</a>

# Development of a shooting machine for the selection of arrows

Masashi Ohara<sup>1</sup> , Naoki Kawasaki<sup>1</sup>, Hyunwoo Song<sup>1</sup> ,  
Ayane Shinojima<sup>2</sup>, Yuma Naka<sup>1</sup>, Yogo Takada<sup>1</sup>  
and Hitoshi Watanabe<sup>3</sup>

Proc IMechE Part P:  
*J Sports Engineering and Technology*  
1–10

© IMechE 2022

Article reuse guidelines:

sagepub.com/journals-permissions

DOI: 10.1177/17543371221141779

journals.sagepub.com/home/pip



## Abstract

It is important to select reliable tools that archers should use in archery competitions. For this reason, we focused on the arrows among the tools and developed a shooting machine for selecting arrows. It is important to imitate the movement of the right finger to release the arrow and the forward movement of the bow after the arrow is released. Therefore, these factors were considered when designing the machine. In this study, a shooting experiment was conducted in which the shooting cycle of twelve ends of six arrows was repeated five times (one end is defined as six arrows). Next, using the data from the impact points on the target, specific arrows with a large dispersion were identified. Cluster analysis was then conducted to identify the arrows that showed a high similarity distribution. Based on the above results, we were able to identify arrows with the most flaws and select arrows that archers should use. The results indicate the effectiveness of the method of selecting reliable arrows by rejecting flawed arrows.

## Keywords

Archery, archer, archery player, arrow, shooting machine, arrow selection, olympic games, cluster analysis

Date received: 1 February 2022; accepted: 9 November 2022

## Introduction

Archery has been adopted as an official sporting event in the Olympics. In addition, numerous archers in Japan have demonstrated excellent performance in championship events in recent years. They are expected to win medals in the upcoming Olympics. In anticipation of the next Olympic games, the All-Japan Archery Federation has begun providing technical support to archers.

Thus, much research has been conducted on archery equipment so that archers can participate in matches with confidence and without anxiety regarding the equipment they use. For example, dynamic and static analyses have been conducted for bows.<sup>1–4</sup> In addition, research has been conducted to clarify the aerodynamic characteristics and behaviors of arrows.<sup>5–12</sup> Moreover, it is necessary to develop a shooting machine for evaluating arrows by shooting them; this research is being actively conducted. For example, Jun et al.<sup>13</sup> used a shooting machine to study the aerodynamic characteristics of arrows. Lin et al.<sup>14</sup> used a shooting machine to study the relationship between the position of the feathers on an arrow and its speed. Moreover, Kormushev et al.<sup>15</sup> developed iCub, a humanoid robot for shooting arrows. However, as iCub can only shoot at a distance

of less than 70 m, it is not suitable as a device for the Olympic Games, where the competition is held at a distance of 70 m. In research overseas, Park et al.<sup>16–18</sup> used a shooting machine to study the aerodynamic drag and axial rotation of arrows as well as the relationship between arrow straightness and the deviation of the impact points on the targets. However, these studies only considered compound bows. Lau et al.<sup>19</sup> experimented on variable lateral bow angles (bow cants) using a shooting machine from a distance of 70 m, but they did not consider the archer's paradox. The archer's paradox is a phenomenon in which an arrow vibrates in a horizontal plane after it has been released owing to the release of the bowstring by a person's fingers. This phenomenon is known to affect the impact points on the target.<sup>20–22</sup> Hirano<sup>23</sup> studied a shooting machine

<sup>1</sup>Graduate School of Engineering, Osaka City University, Osaka-shi, Japan

<sup>2</sup>Department of Engineering, Osaka City University, Osaka-shi, Japan

<sup>3</sup>Research Center for Urban Health and Sports, Osaka City University, Osaka-shi, Japan

### Corresponding author:

Masashi Ohara, Graduate School of Engineering, Osaka City University,  
3-3-138 Sugimoto Sumiyoshi-ku, Osaka-shi, 558-8585, Japan.

Email: laughmaker315@outlook.jp

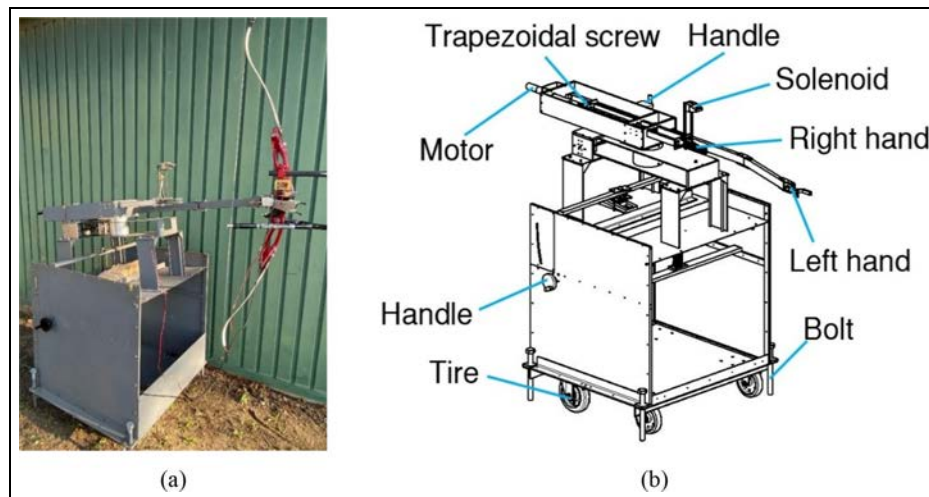


**Figure 1.** Shooting machine: (a) image of the machine and (b) schematic diagram of the machine.

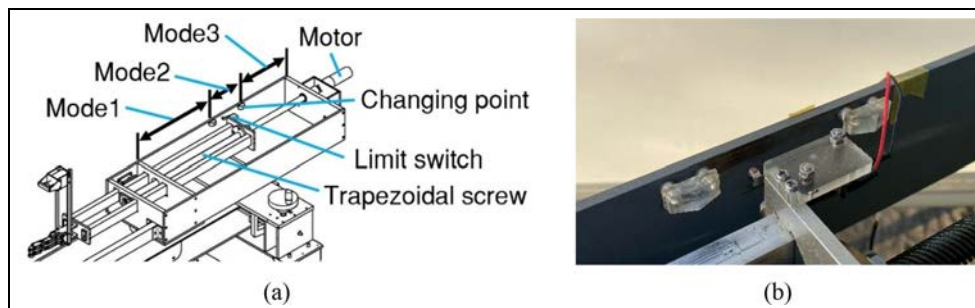


**Figure 2.** System for drawing a bowstring: (a) limit switch used to change each mode and (b) changing points.

that reproduced the archer's paradox. Although this device was successful in recreating the archer's paradox, it only shot at a distance of 30 m. In addition, regarding the left-hand part of the motion, the device was not able to reproduce the forward movement of the bow from the archer's left hand immediately after shooting.

The aim of this study was to select the arrows to be used by archers. To achieve this goal, we developed a shooting machine which is capable of shooting from a distance of 70 m and included a mechanism for imitating the fingers of a person's right hand and the part of the left hand that pushes the bow. The authors developed the first shooting machine between April 2018 and January 2019.<sup>24</sup> However, owing to insufficient stability of the first prototype, they improved it and developed "Shooting Machine 2."<sup>25</sup> In the following text, we refer to "Shooting Machine 2" as the "Shooting Machine." In this study, we conducted shooting experiments to determine whether it is possible to select the arrows that archers should use and to confirm the effectiveness of the proposed method.

## Shooting machine

### Base part

An image of the developed shooting machine is shown in Figure 1(a) and a schematic illustration is shown in

Figure 1(b). The method by which this machine shoots an arrow is as follows: The left hand pushes the bow and the fingers of the right hand hold the bowstring. A trapezoidal screw is adjusted by rotating the handle. The right-hand component then moves backward and a bowstring is drawn. Subsequently, the arrow is shot when the right finger is unlocked. In this study, the dimensions of the machine used are 1872 mm × 903 mm × 1607 mm, and the total mass is 114.4 kg. Because the shooting machine used in this study was developed by Ohara et al.,<sup>25</sup> a detailed description of the machine is omitted in this paper.

### Mechanism for drawing a bowstring

The bowstring drawing mechanism is illustrated in Figure 2. After the arrow is set to the string, the string is pulled by a DC motor (Maxon Motor, model number: 367468). A description of the "clicker" is shown below. Recurve bows include a device that assists the archer to obtain a consistent draw length. This usually takes the form of a "clicker," which is a small blade that sits over the arrow while it is drawn and "clicks" against the side of the bow when full draw is reached. In addition, when archers pull their bows, they gradually decrease the pulling speed as the timing of the

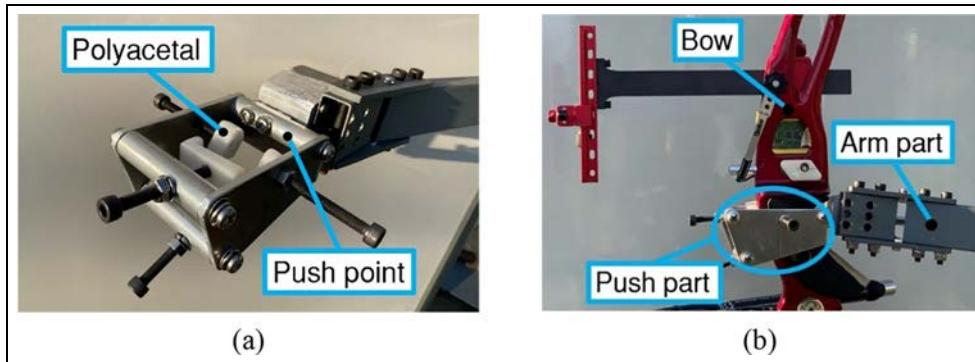


**Figure 3.** Left-arm part: (a) push part and (b) push part with a bow (side view).

clicker drop approaches.<sup>26</sup> Considering this feature, the motor's movements are roughly divided into three modes. Mode 1 includes the rapid drawing of a bow-string; Mode 2 involves deceleration owing to its close proximity to the clicker; and Mode 3 involves further deceleration because the arrow tip will reach the clicker position within seconds.

The length of each mode is determined by adjusting the position of the changing point, as shown in Figure 2(a) and (b), and the positions of these points can be easily changed. Therefore, it can be adjusted and used by any archers with different pull lengths. In this study, the duty ratio of the motor pulse width modulation (PWM) control was set to 30% in Mode 1, 15% in Mode 2, and 10% in Mode 3. These modes are switched by the limit switch, as shown in Figure 2(a) and (b). The limit switch automatically switches when the arrow is pulled.

#### *Left-arm part to push a bow*

The left arm of the machine is made of a square iron pipe with dimensions of 2 mm × 20 mm × 40 mm. Archers in general, utilize the same method for pushing the bow every time. For this reason, the push part of the left hand is designed to always grip the bow so that the bow can be pushed at the same position every time. In this study, we focused on the push aspect rather than the grip aspect and designed the bow to be pushed forward strongly at the push point. The other part of the left hand for fixing the bow is made of polyacetal, as shown in Figure 3(a), allowing the bow to be grasped firmly yet as if it were softly wrapped. If metal had been used to fix the bow, there was a possibility of damaging the archer's bow. However, because polyacetal was used, the bow damage was avoided. Figure 3(b) shows an image of the left hand grasping the bow. Because this machine is designed to be easily detachable, it can be used for all archery bows.

In addition, the push part is connected to the left arm part by a mechanism that is able to slide in the shooting direction. Therefore, when the arrow is shot,

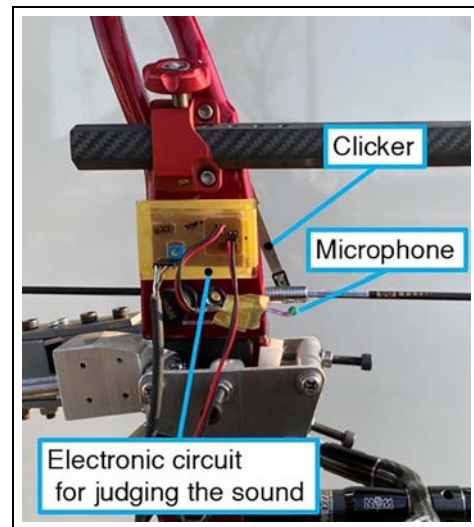


**Figure 4.** Sound judging system.

the push part is designed to slide forward from the arm part while keeping the bow firmly held. This mechanism imitates the motion of the bow being pushed forward from the archer's left hand immediately after shooting the arrow.

#### *Sound judging system*

As mentioned in the previous section, when the tip of an arrow reaches the clicker position, the clicker falls off, and a sound is generated. Then, the human archer would hear the sound and simultaneously shoot the arrow every time. For this reason, a clicker was also used in this study to keep the length of the pull the same each time. In general, clickers are made of aluminum, stainless steel, or carbon; in this study, a stainless steel clicker was used. In previous studies, Ertan et al.<sup>27</sup> placed a conductor metal under a clicker to detect the timing of a clicker drop. Edlmann-Nusser et al.<sup>26</sup> used accelerometers to detect the drop. In contrast, in this study, a microphone was used to detect the timing of the clicker drop, as shown in Figure 4, to imitate the way archers use sound to judge timing.



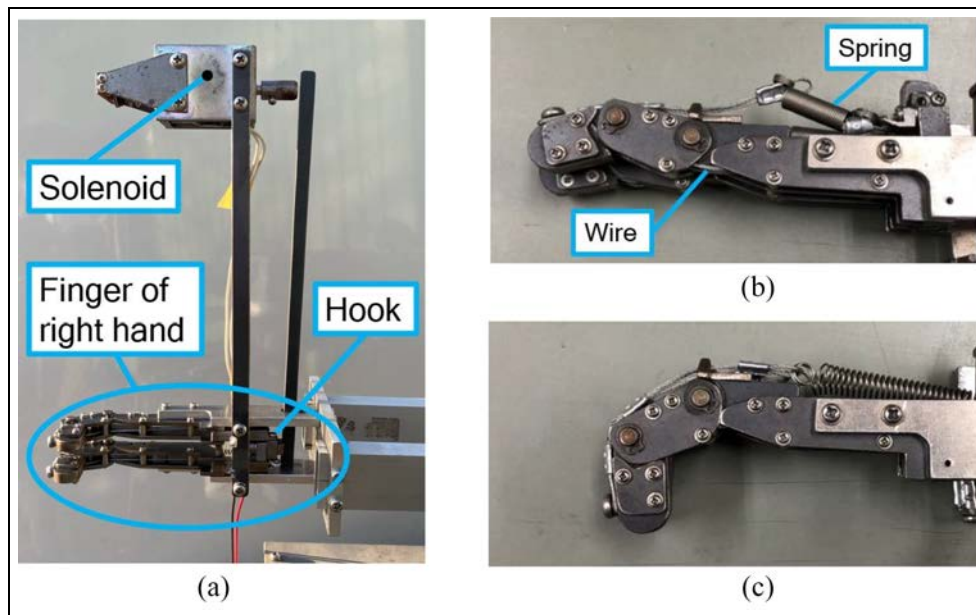


**Figure 5.** Release mechanism: (a) image of the right hand, (b) image of the extended right fingers, and (c) image of the bent right fingers.

### Release mechanism

The image of the right-hand part is shown in Figure 5(a), illustrating the point at which a bowstring can be hooked. The right-hand part of the machine was designed to imitate the fingers of the human hand so that the structure could reproduce the archer's paradox when releasing the arrow. In addition, the bending and stretching of the fingers are performed by pulling wires and springs to resemble the movements of human fingers. Images of the fingers in the extended and bent positions are shown in Figure 5(b) and (c), respectively. In addition, the fingers can be locked in the bent position and extended by applying an electric current to the solenoid when the clicker sound is detected. When the fingers are extended, they move spontaneously by the force of the strings without any particular control.

## Shooting experiment

### Methods

The shooting machine was moved to an archery range, and a shooting experiment was conducted with the aim of selecting arrows. The bow was an INNO CXT made by Win Japan (Osaka City, Japan), and the arrows were X10 shafts made by EASTON (Salt Lake City, United States). The bow weight is 43 lb and the shaft is widely used in the Olympics and other competitions. The type of target was the same as that used in the Olympic Games, with a diameter of 1.22 m. The machine was placed 70 m from the target, and six arrows were used for the experiment. The arrows were numbered from one to six to distinguish them from each other and were released in ascending order. In major world archery

events (the Olympics, World Championships, and World Cup), a ranking round is first conducted. In this round, six arrows are defined as one end, and arrows are then shot for 12 ends. Referring to this standard, in this experiment, we defined six shots as one end and repeated it 12 times for a total of 12 ends. In addition, we defined the 12 ends (72 shots) as one cycle and conducted a total of five cycles in this experiment. Each cycle was distinguished by letters A–E (e.g., Cycle A) to avoid confusion with the numbers used to sort the arrows. The experiment was conducted under the above conditions, and the data on the positions of the impact points on the target were obtained from images captured using a smartphone camera.

### Results

The impact point data of the arrows for the five cycles are shown in Figure 6. The  $x$ -axis and  $y$ -axis indicate the horizontal and vertical distances, respectively, with the average of the impact positions in each cycle as the origin. The arrows were shot toward the east, and the right and left directions in the figure indicate the south and north of the experimental environment, respectively. In addition, the black circle in the figure shows the 10-point area in the archery competition, which has a diameter of 122 mm. This figure also shows a 95% confidence ellipse using the Mahalanobis distance so that the distribution of the arrows can be easily visually understood. The number of each arrow and the color of the corresponding ellipse are shown in the legend. In addition, the date (MM/DD/YYYY) of the experiment is shown next to the cycle name. Based on these results, we consider the following information.

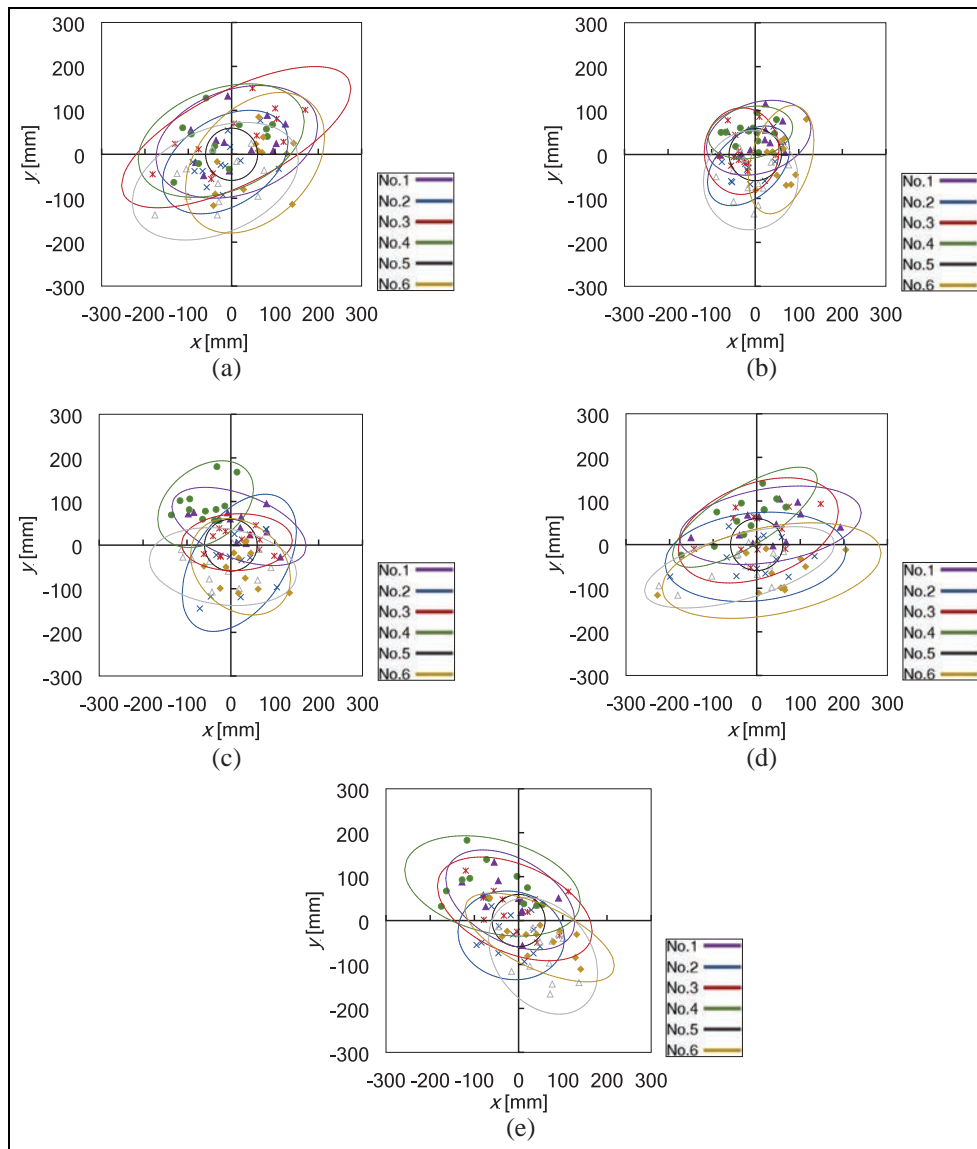


**Figure 6.** Shooting results: (a) Cycle A (10/21/2021), (b) Cycle B (11/04/2021), (c) Cycle C (11/05/2021), (d) Cycle D (11/11/2021), and (e) Cycle E (11/12/2021).

First, in Figure 6(c), the arrow distribution of arrow No. 4 in Cycle C is farther from the vertical direction than the same arrow in the other cycles. In Cycle C, there was a problem at the beginning of the experiment where the arrow nock unexpectedly came off. We reattached the nock in place soon after the incident, but this may have affected the impact points.

Second, Figure 6(d) shows that Cycle D exhibits a large horizontal dispersion. The difference in the scatter of arrows between this cycle and other cycles may be attributed to the effect of a side wind. A specific discussion on side winds is provided in the next section.

## Discussion

In archery matches, two archers compete in elimination matches following the ranking round. In those matches, archers are required to have at least nine

arrows available: three they just shot, three that are still being returned from the target, and three for the next end. Top quality arrows, as used by almost all competitors in an event such as the Olympic Games, usually come as matched sets of 12 arrows. Therefore, in this case, if we can find three arrows with the most faults, we can select 9 out of the 12 arrows that should be used by the archers. In this study, we made an attempt to select three arrows with the most flaws out of six arrows instead of twelve. First, for each arrow, we identified the arrow with the largest dispersion according to the coordinates of the impact points. Next, we analyzed the relationship between the clusters of impact points for each arrow and identified which arrows showed high similarity in terms of distribution. Finally, based on this information, three arrows with the most flaws were identified to confirm the effectiveness of the proposed method.

**Table 1.** Value of corrected  $\sigma'$  for each cycle and each arrow (mm).

	Cycle A	Cycle B	Cycle C	Cycle D	Cycle E	Mean value of $\sigma'$ for each arrow
Arrow No. 1	47.83	30.02	50.63	87.67	37.26	50.68
Arrow No. 2	44.57	23.86	42.47	40.01	50.91	40.36
Arrow No. 3	57.88	34.22	45.29	44.93	59.30	48.32
Arrow No. 4	46.75	32.11	36.56	39.31	41.12	39.17
Arrow No. 5	60.95	47.15	40.73	56.61	43.57	49.80
Arrow No. 6	55.23	26.39	51.64	115.0	60.26	61.71
Mean value of $\sigma'$ for each cycle	52.20	32.29	44.55	63.93	48.74	

**Table 2.** Wind speed data for each experiment day.

		Cycle A	Cycle B	Cycle C	Cycle D	Cycle E
Wind direction data for each hour (during 3 h)	First hour	Southeast	West	North	West-southwest	West-northwest
	Second hour	North-northeast	West-northwest	North-northwest	West-southwest	West-northwest
	Third hour	North-northeast	West	Northwest	West-southwest	West-southwest
Average wind speed (m/s)		1.57	1.17	1.20	4.07	3.50
The average value of deviation (mm)		155	14.5	114	176	152
Maximum wind speed (m/s)		1.90	1.60	1.70	4.80	4.50
The maximum value of deviation (mm)		199	43.4	136	208	195

### Dispersion of arrows

First, we considered the dispersion of the numbered arrows in each cycle. If the data has a normal distribution ( $\sigma$ : standard deviation;  $\mu$ : mean value), the 95% confidence interval is given by ( $\mu \pm 1.96 \sigma$ ).<sup>28</sup> In addition, the impact points of arrows shot by archers are known to be normally distributed.<sup>29</sup> Accordingly, this formula can be applied assuming that the impact points using this machine also have a normal distribution. First, the standard deviation  $\sigma$  of the distance from the origin was calculated. Next, the standard deviation  $\sigma$  was multiplied by 1.96 to obtain  $1.96 \sigma$ . In the following text, we refer to  $1.96 \sigma$  as  $\sigma'$ . The value of  $\sigma'$  for each numbered arrow's cycle and its average values are listed in Table 1. In addition, only a 61 mm radius of the circle, that is, the 10-point region, was used in this study as the evaluation criterion for  $\sigma'$ . The values in Table 1 that exceed this criterion are indicated in red. From this result, it could be seen that arrows No. 1 and No. 6 in Cycle D exceeded 61 mm. Moreover, a comparison of the mean value of  $\sigma'$  for each arrow showed that arrow No. 6 had the largest value, that is, above 61 mm. Therefore, this result suggested that arrow No. 6 was the most flawed among the six arrows and should not have been used by archers. It was also evident that if archers need the most accurate arrow (such as in the case of a match in which the winner or loser is determined by the accuracy of a single shot), they should choose No. 4, which had the smallest mean value of  $\sigma'$ .

Next, we considered why the mean value of  $\sigma'$  for each cycle was different between cycles. The

experiments for each cycle were conducted for approximately 3 h on different days. Table 2 shows the maximum and average wind speeds for the 3 h during our data capture on the experimental day, and the wind direction by each hour at the point closest to the experimental site, as obtained from the Japan Meteorological Agency.<sup>30</sup> According to these data, the wind was strong on the experimental days of Cycles D and E. It was thought that wind had a large effect on the impact points of the arrow, especially when it blew laterally to the arrow. Therefore, calculations were conducted to examine the possible lateral displacement at a distance of 70 m according to the side winds.

In another study, Ortiz et al.<sup>31</sup> conducted a numerical calculation of the lateral displacement caused by a side wind. Although it was difficult to exactly match the conditions of this experiment because of parameters that were difficult to measure, such as the speed of the arrow in flight, we could use the values from their study as an approximation. According to the data, a uniform side-wind with a velocity of 3 m/s resulted in a 340 mm displacement from the center of the target. In addition, the equation used in the study showed that there was a proportional relationship between the side wind and displacement. Table 2 shows the values of the average lateral displacement and maximum assumed lateral displacement in this experiment, which were calculated using the data from the study mentioned above and the wind speed data from our experiment. In this calculation, we considered the wind direction and assumed that only the wind velocity components in the north

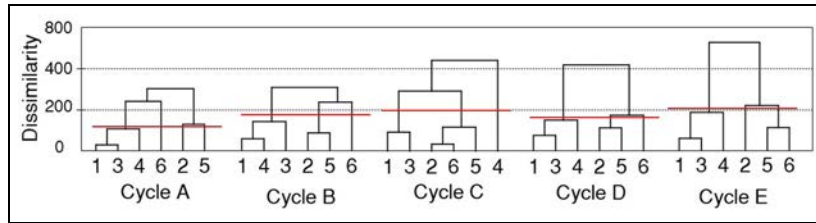


**Figure 7.** Cluster analysis for each cycle.

and south directions affected the arrows because the arrow was shot eastward. In addition, the deviation was calculated as an absolute value, with no positive or negative values defined for the north and south directions. The theoretical value of the lateral displacement calculated from the data in this study was quite large because it was calculated in a case where the wind was always blowing, unlike in the actual experimental environment. However, the results demonstrated that if a strong wind blew at the time of shooting the arrows, a large displacement was observed. Moreover, this result also showed that there was a reasonable possibility of large differences between cycles performed on strong-wind days and light-wind days.

### Cluster analysis

After focusing on dispersion, we analyzed the impact points in each cycle separately to examine the distribution of the arrows. In this study, we applied a hierarchical clustering method that has been used in many fields.<sup>32,33</sup> First, the arrows marked with the same number were combined to form clusters, and then the similarity between clusters was considered. In cluster analysis, there are many ways to determine the distance between a cluster formed by combining two clusters with other clusters. In this study, we applied the Ward method, which is known to be more robust to outliers than other methods.<sup>34,35</sup> Incidentally, the Ward method combines two clusters to maximize the ratio of the variance within the group to that between the groups. Additionally, the distance between each impact point was calculated using the Euclidean square distance. Dendrograms created based on the analysis results are shown in Figure 7. In the dendrogram, the horizontal axis shows the number marked on the arrow in each cycle, and the vertical axis shows the distance between the clusters, as obtained by the calculation. In the figure, the square root of the calculated value is shown because the Euclidean square distance is used for the distance calculation. Moreover, this distance represents the dissimilarity between clusters. This means that the clusters joined at a lower position in the dendrogram have a higher similarity, indicating that they are clusters of arrows with similar characteristics. Then, red lines are marked on the branches at the points where a cluster containing three or more arrows has been combined. The branches are the lines connecting each element in the dendrogram.

From this result, it could be concluded that, with the exception of Cycle C, the clusters could be classified into those containing arrows No. 1, 3, and 4 and those containing arrows No. 2, 5, and 6. As for arrow No. 4 of Cycle C, the impact points were distributed vertically upward owing to an accident in which thenock unexpectedly missed once, as noted in the results section. Thus, it was thought that the classification result of Cycle C was different from those of the other cycles because of this effect, as shown in the dendrogram. However, the average value of the dispersion of arrow No. 4 was small, as shown in Table 1. Moreover, because this was the only day in which the arrows dispersed in significantly deviated positions, we considered it unlikely that there was any flaw in this arrow. Furthermore, it could be considered that arrows No. 1 and 3 were the two most similar arrows among the six arrows because these two arrows form the cluster initially in three cycles (Cycle A, D, and E). In addition, arrow No. 6 had the highest dispersion degree among the six arrows shown in Table 1, indicating that this arrow had the most flaws. Based on the above considerations, it was concluded that among these six arrows, arrows No. 2, 5, and 6 should not have been used, whereas arrows No. 1, 3, and 4 should be used by archers. In this experiment, three arrows with most flaws were rejected from six arrows. Then, even with 12 arrows in the actual case, using the same method, it would be possible to reject the three arrows with most flaws and select nine arrows that should be used.

Next, in order to consider the effect of wind, we performed cluster analyses using the dispersions in each direction separately. The dendrograms obtained using only the horizontal dispersion are shown in Figure 8, and those obtained using only the vertical dispersion are shown in Figure 9. In these analyses, we also applied the Ward method for each cycle.

We discuss Figure 8, in which only horizontal dispersion is considered. These results had no similarities between each cycle, and we cannot select the arrows. Then, we discuss Figure 9, in which only vertical dispersion is considered. These results suggested that, with the exception of Cycle B, the clusters could be classified into those containing arrows No. 1, 3, and 4 and those containing arrows No. 2, 5, and 6. In addition, Table 1 showed that arrow No. 6 had the highest dispersion degree among the six arrows. Therefore, it was concluded that arrows No. 2, 5, and 6 were the arrows that



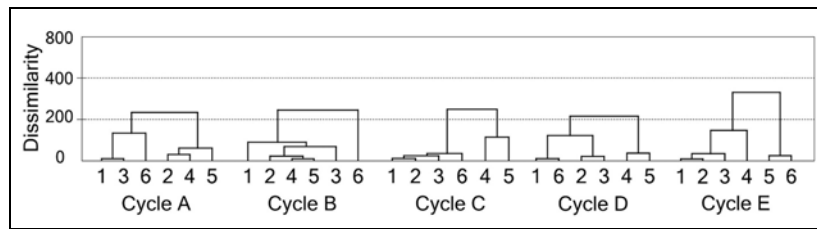


**Figure 8.** Cluster analysis for each cycle using only horizontal dispersion.

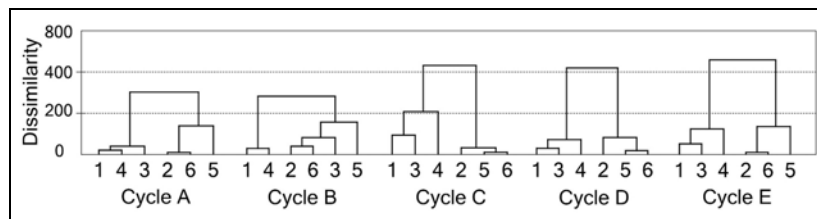


**Figure 9.** Cluster analysis for each cycle using only vertical dispersion.

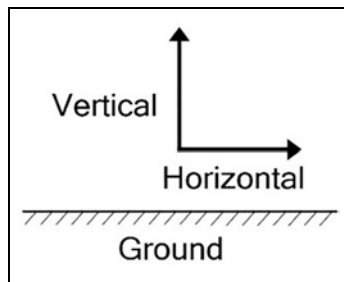


**Figure 10.** Definition of wind direction.

**Table 3.** Horizontal and vertical wind speeds relative to the ground at archery range.

The distance from the target (m)	30	50	70
Horizontal wind speed (m/s)	2.2	2.7	2.1
Vertical wind speed (m/s)	0.0	0.6	0.0

archers should not use, and arrows No. 1, 3, and 4 are the arrows that archers should use. By comparing the dendrograms using only vertical dispersion with those in Figure 7, it was shown that the classification results for Cycle B in Figure 9 and Cycle C in Figure 7 are different. However, the selection results obtained considering all five cycles were the same for No. 1, 3, and 4.

Next, we describe the wind speeds measured with the anemometer at the archery range where the experiment was conducted. As shown in Figure 10, wind speeds in the horizontal and vertical directions relative to the ground were measured. These values, measured at distances of 30, 50, and 70 m from the target, are shown in Table 3. This table indicated that the wind blew mostly horizontally, and the vertical wind blew very little and influenced arrows little.

From these results, the reason for the inability to select arrows from the results using only the horizontal

dispersion was the effect of the crosswind. It was then clarified that the results using only vertical dispersion, which were less influenced by wind, provide the same conclusion as those obtained by considering both horizontal and vertical dispersion. This indicated that it was possible to select arrows even with the current equipment. However, to conduct more accurate analysis regarding the horizontal direction, it is necessary to conduct the experiment where the wind has less influence.

## Conclusion

In this study, a shooting machine was developed to select the arrows that should be used by the archer, and shooting experiments were conducted using the six arrows actually used by archers. Archers participating in the Olympics need to identify 3 arrows from 12 with most flaws and reject them to select nine arrows to be used in a match. Therefore, in this study, we identified three flawed arrows out of six to verify the effectiveness of this method. In the arrow shooting experiment, six arrows were shot as one end according to the rules of the ranking round, and 12 ends (72 shots) were shot in total, which were repeated for five cycles.

Subsequently, we first identified the specific arrows likely to have most flaws by using the standard deviations calculated from the impact points of the arrows. Second, cluster analysis was conducted separately for each cycle, and arrows showing a high similarity distribution were identified. Based on the information provided above, we were able to identify three arrows out of six that had significant flaws and should not be used by the archer. These results indicated that even with 12 arrows, as in the competition setting, using the same method it would be possible to select nine arrows that should be used, rejecting the three arrows with high degree of flaws.

As future problems, the effects of side winds on the arrows are significant, and it is difficult to accurately detect the unique dispersion of arrows on a windy day. Therefore, we will conduct further experiments in an environment where there is no external influence, such as wind.


### Declaration of conflicting interests


The author(s) declared no potential conflicts of interest with respect to the research, authorship, and/or publication of this article.

### Funding

The author(s) received no financial support for the research, authorship, and/or publication of this article.

### ORCID iDs

Masashi Ohara  <https://orcid.org/0000-0003-3245-3541>

Hyunwoo Song  <https://orcid.org/0000-0002-9840-1923>

### References

- Marlow WC. Bow and arrow dynamics. *Am J Phys* 1981; 49: 320–333.
- Park JL. A compound archery bow dynamic model, suggesting modifications to improve accuracy. *Proc IMechE Part P: J Sports Engineering and Technology* 2009; 223: 139–150.
- Zanevskyy I. Modeling and computer simulation of bow stabilization in the vertical plane. *Int J Sports Sci Eng* 2008; 02: 3–14.
- Zanevskyy I. Compound archery bow asymmetry in the vertical plane. *Sports Eng* 2012; 15: 167–175.
- Miyazaki T, Mukaiyama K, Komori Y, et al. Aerodynamic properties of an archery arrow. *Sports Eng* 2013; 16: 43–54.
- Park JL, Hodge MR, Al-Mulla S, et al. Air flow around the point of an arrow. *Proc IMechE Part P: J Sports Engineering and Technology* 2013; 227: 64–69.
- Yong WF, Ahmad Z and Sahat IM. Development and analysis of arrow for archery. *J Eng Appl Sci* 2016; 11: 7443–7450.
- Park JL. The behaviour of an arrow shot from a compound archery bow. *Proc IMechE Part P: J Sports Engineering and Technology* 2011; 225: 8–21.
- Rieckmann M, Codrington J and Cazzolato B. Modelling the vibrational behaviour of composite archery arrows. In: *Proceedings of ACOUSTICS, Gold Coast, Australia*, 2–4 November 2011, paper no. 102, pp.1–8. Australia: AAS.
- Rieckmann M, Park JL, Codrington J, et al. Modelling the three-dimensional vibration of composite archery arrows under free-free boundary conditions. *Proc IMechE Part P: J Sports Engineering and Technology* 2012; 226: 114–122.
- Park JL. The impact of the atmosphere on target archery. *Proc IMechE Part P: J Sports Engineering and Technology* 2019; 235: 251–256.
- Park JL. Arrow behaviour in free flight. *Proc IMechE Part P: J Sports Engineering and Technology* 2011; 225: 241–252.
- Jun W, Chisato K, Ryu A, et al. Development of archery robot: development of finger mechanism for controllable the bending vibration. In: *JSME conference on robotics and mechatronics*, Kyoto, Japan, 17–19 May 2015, paper no. 2A2-T08, pp.1–3. Japan: JSME.
- Lin K, Huang K-S, Hwang C-K, et al. Performance analysis based on an emulated archery machine. In: *Proceedings of the eighth international conference on machine learning and cybernetics*, Baoding, China, 12–15 July 2009, pp.3275–3278. Germany: dblp.
- Kormushev P, Calinon S, Saegusa R, et al. Learning the skill of archery by a humanoid robot iCub. In: *2010 IEEE-RAS international conference on humanoid robots*, Nashville, TN, 6–8 December 2010, pp.417–423. New York: IEEE.
- Park JL, Aitchison PJ, Bielby AJ, et al. Effect of arrow shaft straightness on arrow grouping. *Proc IMechE Part P: J Sports Engineering and Technology* 2017; 232: 236–241.
- Park JL. Minimizing wind drift of an arrow. *Proc IMechE Part P: J Sports Engineering and Technology* 2011; 226: 52–60.
- Park JL. The aerodynamic drag and axial rotation of an arrow. *Proc IMechE Part P: J Sports Engineering and Technology* 2011; 225: 199–211.
- Lau M, Chung H, Park JL, et al. A device for measuring the variable lateral bow angle and its impact on score loss. *Proc IMechE Part P: J Sports Engineering and Technology* 2018; 233: 362–369.
- Kooi BW and Sparenberg JA. On the mechanics of the arrow: archer's paradox. *J Eng Math* 1997; 31: 285–303.
- Kooi BW. Bow-arrow interaction in archery. *J Sports Sci* 1998; 16: 721–731.
- Itoh T and Takaoka M. *Regulations and dynamical model for bow-arrow system and finger release in archery paradox*. The Science and Engineering Review of Doshisha University, Doshisha University, Japan, April 2009; 50(1): 1–8.
- Hirano T. *Production and performance evaluation of archery shooting machine reproducing paradox*. Bulletin of Science and Engineering, Takushoku University, Japan, March 1993; 18: 27–31.
- Nakamura T, Takada Y and Watanabe H. Statics investigation about archery robot in drawing a bow. In: *Proceedings of the 2019 JSME conference on robotics and mechatronics*, Hiroshima, Japan, 5–8 June 2019, paper no.1P1-Q06. Japan: ASME.
- Ohara M, Kawasaki N, Nakahama J, et al. Development of an archery robot for the selection of arrows. In: *The 13th conference of the international sports engineering association*, Online, 22–26 June 2020, paper no. 49-115, pp.1–7. UK: ISEA.
- Edelmann-Nusser J, Heller M, Hofmann M, et al. On-target trajectories and the final pull in archery. *Eur J Sport Sci* 2006; 6: 213–222.
- Ertan H, Kentel BB, Turgut Tümer S, et al. Reliability and validity testing of an archery chronometer. *J Sports Sci Med* 2005; 4: 95–104.
- Bewick V, Cheek L and Ball J. Statistics review 7: correlation and regression. Review, BioMed Central Ltd, UK, November 2003.
- Park JL. The relative performance levels of archers in ranking rounds and matches. *Proc IMechE Part P: J Sports Engineering and Technology* 2020; 235: 29–35.

30. Japan Meteorological Agency, <https://www.data.jma.go.jp/obd/stats/etrn/index.php> (2021, accessed 31 December 2021).
31. Ortiz J, Ando M, Murayama K, et al. Computation of the trajectory and attitude of arrows subject to back ground wind. *Sports Eng* 2019; 22: 1–9.
32. Romesburg HC. *Cluster analysis for researchers*. 1st ed. Japan: Uchida Rokakuho, 1992, pp.369–376.
33. Beckmann M and Künzi HP. *Lecture notes in economics and mathematical systems*. 1st ed. Germany: Springer Berlin Heidelberg, 1974, pp.104–109.
34. Saito T and Yadohisa H. *Analysis of relational data-multidimensional scaling and cluster analysis*. 1st ed. Japan: Kyoritsu Shuppan, 2006, pp.137–140.
35. Anderberg MR. *Cluster analysis for applications*. 1st ed. San Diego, CA: Academic Press, 1973, pp.142–145.